Hindawi
Advances in Civil Engineering
Volume 2023, Article ID 9451361, 13 pages
https://doi.org/10.1155/2023/9451361

Research Article

Influence of Segmented Linings on the Micro-Pressure Wave of Tunnels

Tao Li,[1] **Mingyu Shao**,[1] **Weibin Ma**,[2] **Yanbin Liang**,[1] **and Yufei Fang**[2]

[1]*School of Transportation and Vehicle Engineering, Shandong University of Technology, Zibo 25000, China*
[2]*State Key Laboratory for Track Technology of High-speed Railway, Beijing 100081, China*

Correspondence should be addressed to Mingyu Shao; shaomingyu@sdut.edu.cn

Received 25 August 2022; Accepted 5 October 2022; Published 17 February 2023

Academic Editor: Chao Zou

When the tunnel has damages such as deformation and cracking, the lining structure should be set to reinforce the tunnel. In this study, a three-dimensional numerical method is performed to study the aerodynamic effects caused by the train passing through a tunnel with segmented linings at 350 km/h. The influence of the numbers, thickness, location, and types of the segmented lining structure on MPW is analyzed. The results show that the segmented linings located at the middle of the tunnel have a better mitigation effect on MPW than that of the normal linings, which increases with the segment number and the thickness of the linings. When the damage occurs near the entrance of the tunnel, a segmented lining structure with a constricted section slightly away from the tunnel entrance can be used to reduce its adverse effect on MPW.

1. Introduction

The impact of aerodynamic effects caused by high-speed trains entering tunnels increases with the speed-up of trains. Compression waves produced generated when the high-speed train enters a tunnel propagate along the tunnel near to the sonic speed and create a pulse wave at tunnel exits, usually called micro-pressure wave (MPW) [1]. The MPW causes problems such as noise pollution and even a sonic boom, which can lead to structural damage to the buildings surrounding the tunnel exit and negatively affect residents' normal lives [2–4]. Wide research has shown that assessing MPW and structural vibrations are associated with safety and discomfort caused in trains [5, 6]. Zou et al. developed an efficient computational model that can accurately predict over-track vibration levels for buildings supported on a transfer structure [7].

The train speed and blockage ratio are significant factors that affect the amplitude of MPW [8–13]. When the tunnel is under the influence of geology and construction, there are tunnel damages such as structural deformation and cracking [14]. Tunnel damage threatens traffic safety in tunnels and shortens the tunnels' maintenance cycle and service life. Adding linings technology is a popular way to prevent the occurrence or further expansion of cracks. However, adding linings inside the tunnel changes the clearance area and cross-sectional distribution of the tunnel, which affects the aerodynamic characteristics of the tunnel. The lining is to pour a certain thickness of reinforced concrete in the tunnel to prevent the tunnel from further cracking, damage, and deformation. Jin et al. studied the feature morphology of rubberized concrete by corrosion and expansion of reinforcement in rubberized concrete and the relationship between the deformation of staggered assembled shield tunnel and the disengaging of invert filling [15, 16].

Previously many researches were concentrated on the responses of the tunnel hood to MPW of the tunnel. Tunnel hood is an auxiliary structure specifically designed to reduce the impact of tunnel aerodynamics. Xiang et al. compared different tunnel entrance hoods and optimized hood designs to mitigate the pressure gradient [17]. Murray's theoretical research on the tunnel entrance hoods show that the installation of the tunnel hoods will increase the rise time of the initial compression wave, thereby decreasing the

pressure gradient [18]. Studies nowadays have contributed extensively to designing optimized tunnel hoods to reduce the amplitude of MPW at the tunnel exit [19–23]. Although related studies have been performed on the influences of tunnel hoods, limited investigations have been conducted on the effects of MPW behaviors of the linings. Based on the real vehicle experiments, dynamic model experiments, and numerical simulations method to analyze the aerodynamic effects of the train passing the tunnel with linings, Liu et al. pointed out that the influence of MPW is the most unfavorable when the linings are added at the tunnel entrance and the pressure amplitude increases with the thickness of the linings [24, 25]. Combined with the test results of the real vehicle, Gao found MPW and the comfort of the tunnel when the train passed through the lined tunnel and proposed that the impact section of the linings should not exceed 95% [26]. Shi et al. investigated the influence of linings length, thickness, and position on the pressure gradient at the tunnel exit through 3D numerical simulation and found that the impact of linings thickness was more significant than that of length [27]. Wang et al. analyzed the transient pressure characteristics of trains passing through tunnels with noncircular linings based on dynamic model experiments. The results show that reasonable distribution of circular linings can reduce the pressure amplitude of initial compression waves [28].

The above research has shown that adding a lining structure at the tunnel's entrance will adversely affect MPW, but the damage may occur anywhere in the tunnel. Therefore, the behaviors of the aerodynamic effect of the segmented lining structure are assessed in this study. In Section 2, the governing equations and mesh motion equations of the train moving in the tunnel are presented. In Section 3, the numerical calculation model of the train tunnel was established and validated with the dynamic model experiments. In Section 4, the influence of the linings' position, thickness, number of segments, and types on MPW characteristics of the tunnel exit was discussed. The results can provide a fundamental comprehension and reference to the design of the lining structure.

2. Numerical Calculation Method

2.1. Governing Equation. The flow field, produced by trains traveling through the tunnel, is 3D, viscous compressible, and turbulent [9, 29–31], which must follow the laws of continuity equations, momentum equations, and energy equations [32]. They can be written as

$$\begin{aligned}
&\frac{\partial p}{\partial t} + \frac{\partial}{\partial x_i}(\rho u_i) = 0 \\
&\frac{\partial}{\partial t}(\rho u_i) + \frac{\partial}{\partial x_j}\left(\rho u_i u_j\right) = -\frac{\partial p}{\partial x_i} + \rho g \delta_{i2} + \frac{\partial}{\partial x_j}\left[\mu\left(\frac{\partial u_i}{\partial x_j} + \frac{\partial u_j}{\partial x_i} - \frac{2}{3}\delta_{ij}\frac{\partial u_i}{\partial x_i}\right)\right] + \frac{\partial}{\partial x_j}\left(-\rho\overline{u_i u_j}\right) \\
&\frac{\partial}{\partial t}(\rho E) + \frac{\partial}{\partial x_i}\left[u_i(\rho E + p)\right] = \frac{\partial}{\partial x_j}\left(K\frac{\partial T}{\partial x_j} + u_i \tau_{ij}\right),
\end{aligned} \tag{1}$$

where ρ is the density of the air; u_i and u_j are the velocity components in the three directions of the flow field; x_i and x_j are the three components of the coordinate; p denotes the pressure; τ_{ij} is the shear stress in the flow field; K is the thermal conductivity coefficient; T is the temperature of the flow field; and μ is their dynamic viscosity of the air.

The term $-\rho\overline{u_i u_j}$ is the time-averaged Reynolds stresses which represent the turbulent momentum fluxes. Based on the Boussinesq hypothesis, the closed equations under the Boussinesq hypothesis:

$$-\rho\overline{u_i' u_j'} = \mu_t\left(\frac{\partial u_i}{\partial x_j} + \frac{\partial u_j}{\partial x_j}\right) - \frac{2}{3}\left(\rho\kappa + \mu_t\frac{\partial u_\kappa}{\partial x_\kappa}\right)\delta_{ij}, \tag{2}$$

where μ_t is the turbulent viscosity and κ is the turbulent kinetic energy.

The dynamic mesh method is usually accustomed to simulate the time-varying flow on domain boundaries due to train motion in tunnels. The motion can be a prescribed motion or an unprescribed motion which is determined based on the solution at the current time.

Generally, the integral form of the conservation equation for a general scalar, ϕ, on an arbitrary control volume, V, whose boundaries are moving, can be written as [31, 33]

$$\frac{d}{dt}\int_V \rho\phi\, dV + \int_{\partial V}\rho\phi\left(\vec{u} - \vec{u}_g\right)d\vec{A} = \int_{\partial V}\Gamma\nabla\phi\, d\vec{A} + \int_V S_\phi dV. \tag{3}$$

For solving (3), the differential term is discretized as follows:

$$\frac{d}{dt}\int_V \rho\phi\, dV = \frac{(\rho\phi V)^{n+1} - (\rho\phi V)^n}{\Delta t}, \tag{4}$$

where n and $n+1$ represent the value at the present and next time step. The $(n+1)th$ time step control volume, V^{n+1}, is computed from

$$V^{n+1} = V^n + \left(\sum_f^{nf} \frac{\delta V_j}{\Delta t}\right)\Delta t. \tag{5}$$

These equations can then be solved using dynamic meshing methods and updated with new volumes at each time step.

2.2. Computational Model. In this study, the CR400AF vehicle depicted in Figure 1(a) is selected to research the aerodynamic impact of the tunnels with segmented linings. Since the initial compression wave and MPW are mainly associated with the shape of the train nose, four-car marshaling carriages are modeled to improve computational efficiency. The shape of the train is simplified according to the recommendations of the CEN European Standard [34], as the accessory components of the high-speed train (such as pantograph, bogie, doors, and windows) have negligible influence on MPW. According to Chinese high-speed railway tunnel design standards, a double-track tunnel with a cross-sectional area of 100 m^2 is adopted for a high-speed train with a design speed of 350 km/h, and the centre-to-centre distance of the two tracks is 5 m. The cross section size of the tunnel is shown in Figure 1(b), and the length of the tunnel is 1000 m. Different numbers of segmented linings with various thicknesses are set within a certain length of 100 m at different locations of the tunnel to investigate the influences of the segmented linings on MPW, as shown in Figure 1(c).

2.3. Computational Domain and Boundary Conditions. The computational domain of the aerodynamic impacts generated by the trains traveling from the tunnel with segmented linings is composed of the atmosphere outside the tunnel portal and the atmosphere inside the tunnel, shown in Figure 2. Considering the acceleration process of the train and the full development of the wake [35], the length of the flow field outside the tunnel is taken as 500 m on both sides of the tunnel.

The train motion in the tunnel is simulated by the sliding mesh model and mesh dynamic layering method, so the entire computational domain is divided into four domains [30, 36]: a motion domain (region-2), two deformation domains (region-1 and region-3), and a fixed domain (region-4). As the train moves at speed as the surrounding motion domain, the lengths of deformation domains are changed to keep the entire computational domain unchanged during computation. *Interface* boundary conditions are used between the motion domain, the deformation domain, and the fixed domain to realize data exchange. The boundaries of the flow field outside the tunnel portal are defined as *pressure inlet* and *pressure outlet*, respectively. *No-slip wall* is defined as the train surface, ground, and tunnel wall. All walls are defined as *Adiabatic wall* with an initial temperature of 300 K.

2.4. Grid Generation Scheme. A hybrid grid scheme is adopted to divide the entire computational domain into blocks accounting for computational accuracy and speed [37]. The unstructured grid is used in the motion domain surrounding the train as the complicated shape of the train, and the geometrically complex parts of the train surface are locally refined. The deformation domains before and after the motion domain can be divided into high-quality structured grids, and the adjacent regions are connected by setting common nodes on the interface with the motion domain. The structured grid is also used in the fixed domain, and the regions near the segmented linings are refined to capture the influence of the local flow field on the MPW.

In order to evaluate the mesh density on the numerical results, four different grid numbers were taken into consideration, which are 3.98×10^6, 5.19×10^6, 6.60×10^6, and 8.12×10^6, respectively. The details of grids and the amplitude values of MPW calculated by 4 different numbers of grids are shown in Table 1. The results show that the amplitude values of MPW are very little when the number of the grids exceeds 5.19×10^6, which means that the computational accuracy and efficiency can be met when the mentioned mesh is used. In such cases, the grid of the train head and segmented linings are shown in Figure 3.

2.5. Measuring Points. The evaluation standard of MPW at the tunnel exit of a high-speed railway is that the amplitude values of MPW at 20 m and 50 m away from the tunnel exit are less than 50 Pa and 20 Pa, respectively [22].

Studies show that the magnitude of MPW emitting from the tunnel exit is almost proportional to pressure gradients of the wavefront of the initial compression wave reaching the tunnel exit and inversely proportional to the distance to the tunnel exit plane [38], which can be expressed as follows:

$$P_{MPW}(r,t) = \frac{2S}{\Omega c r}\left(\frac{\partial p}{\partial t}\right), \tag{6}$$

where S is the cross-sectional area of the tunnel exit, Ω denotes the solid angle around the tunnel exit portal, c is the speed of sound, r is the distance from the measuring point to the tunnel entrance, and $(\partial p/\partial t)$ demotes the pressure gradient at the tunnel exit.

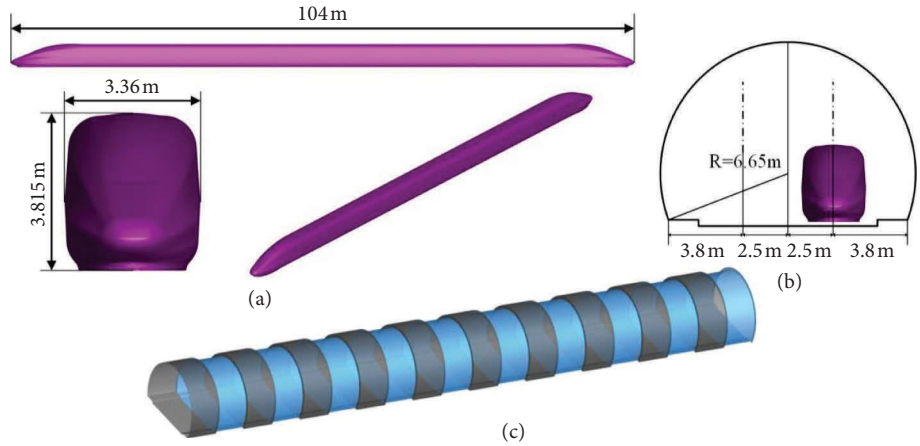

Figure 1: Schematic diagram of models. (a) Different views of CR400AF. (b) Tunnel section. (c) Linings.

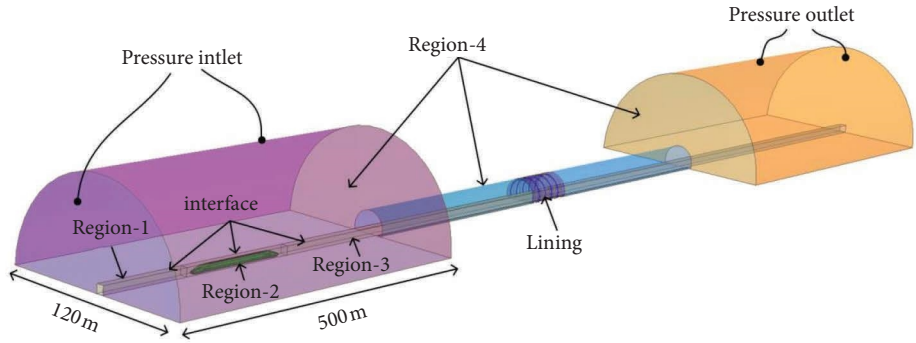

Figure 2: Computational domain and boundary conditions.

Table 1: Grid quantity and micropressure wave.

Grid quantity	3.98×10^6	5.19×10^6	6.60×10^6	8.12×10^6
MPW	72.0	68.4	68.1	67.5

Both the pressure gradient near the tunnel exits and MPW outside the tunnel are monitored simultaneously in the calculation. Two groups of monitoring points 1.2 m above the ground are arranged symmetrically on both sides of the tunnel centreline, as shown in Figure 4. The monitoring point located at 50 m inside the tunnel is marked as $T1$ and $T2$, and $M1,2$ and $M3,4$ denote the monitoring points located at 20 m and 50 m outside the tunnel, respectively.

3. Numerical Method Validation

To verify the accuracy of the presented method in the simulation, the numerical results are compared with that of the moving model test conducted by Central South University [39]. The model ratio in the test is 1 : 20, and the original lengths of the train and the double tracks tunnel are 51.7 m and 1000 m, respectively. A ring tunnel portal with a slope value of 1 : 1.25 is set at tunnel entrance. Both the transient pressure at 65.5 m from the entrance in the tunnel and MPW at 20 m from the exit outside the tunnel are measured in the test when the train passes the tunnel at 350 km/h. The numerical simulation is performed in the same condition as the moving model test.

ANSYS Fluent is used to explain the governing equation of flow motion. The ideal gas model is adopted in the calculation, and the *RNG k-ε* turbulence model is used due to the high turbidity. The coupling velocity and pressure are dealt with the *SIMPLE* algorithm, the gradient term is discretized by the *Green-Gaussian Cell-Based* method. The pressure term is discretized using the standard format, the other spatial terms are discretized by the second-order upwind format and the second-order implicit format is used in the time discretization.

The initial compression wave and MPW acquired by the numerical simulation and moving model tests are shown in Figure 5. It can be seen that the results calculated by the numerical method agree well with those of the moving model test. The amplitude values of MPW and the pressure gradient of the initial compression wave are also listed in Table 2. Because the numerical calculation model has assumptions and errors in the calculation process, the results of the numerical method are not exactly the same as those of the moving model test. The differences between the results from the numerical method and that of the moving model test are 2.86% and 2.60%, respectively. The results show that the numerical methods adopted can meet the requirements of calculation accuracy and efficiency. Thus, the mentioned

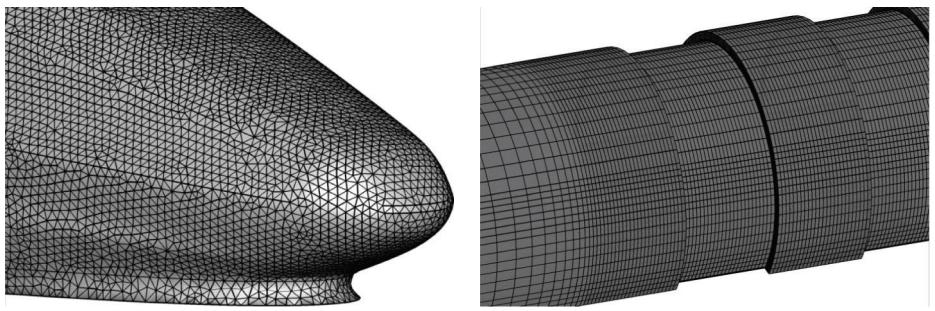

(a) (b)

Figure 3: Model mesh. (a) Mesh of the train head. (b) Mesh of the lining.

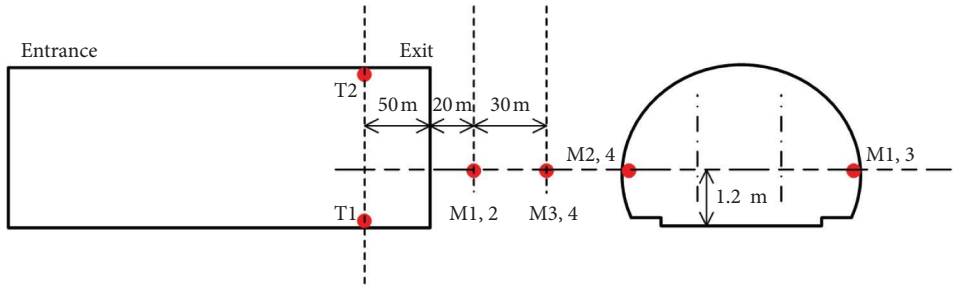

Figure 4: Layout monitoring points.

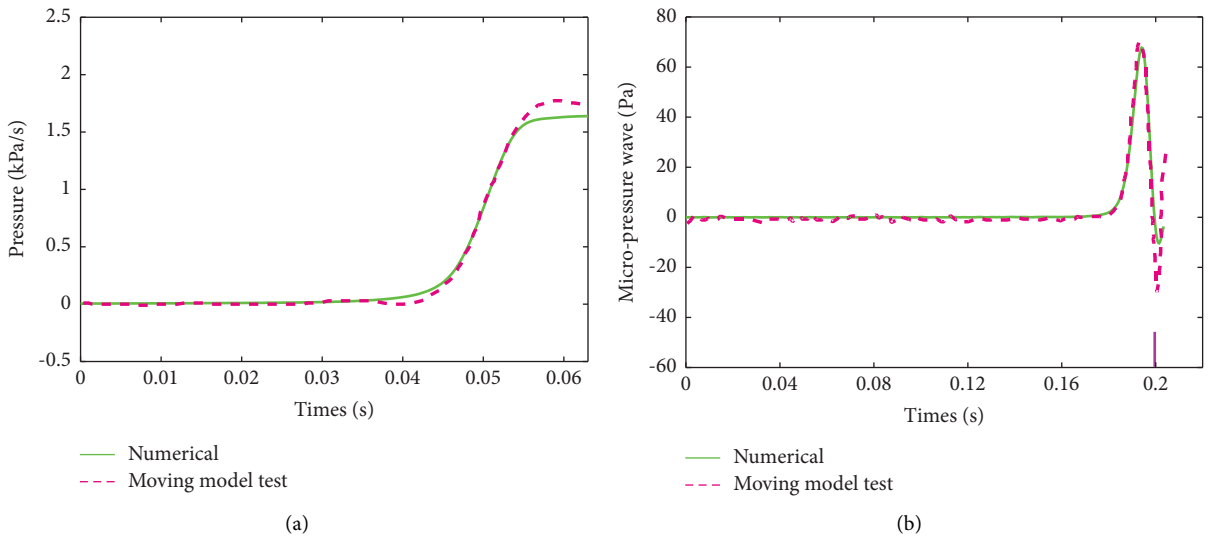

(a) (b)

Figure 5: Comparisons of pressure curves obtained by numerical simulation and the experimental test. (a) Initial compression waves. (b) Micropressure waves.

Table 2: The maximum pressure gradient and the micropressure wave.

	Tests	Numerical	Diff./Ref. (%)
$(\partial P/\partial t)_{max}$ (kPa/s)	9.482	9.729	2.60
MPW (Pa)	70	68	2.86

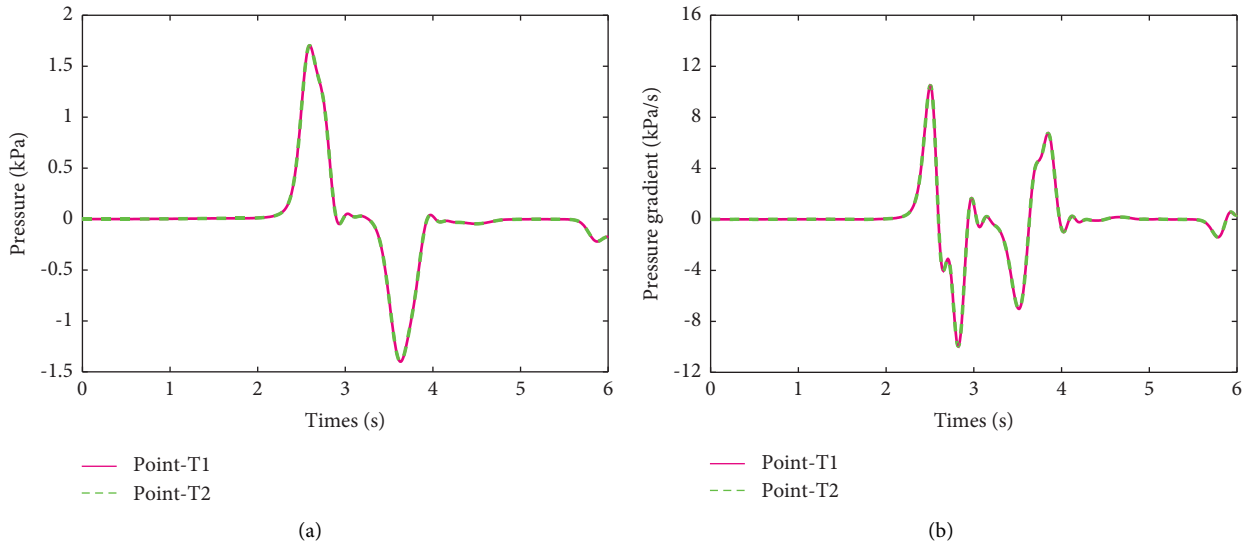

Figure 6: Comparison of initial compression waves in the same plane. (a) Pressure. (b) Pressure gradient.

method in this paper can be used to study the characteristics of MPW caused by the train passing through the tunnel.

4. Results and Discussion

4.1. Propagation Characteristics of Initial Compression Wave. The aerodynamics caused by the train traveling through the tunnel without linings at 350 km/h is simulated by the mentioned method. The comparison of the pressure and pressure gradient of two symmetrical measuring points in the same plane of the tunnel is shown in Figure 6.

It can be found that the results at $T1$ are basically the same as that at $T2$, which indicates that the initial compression wave presents a one-dimensional plane wave characteristic propagating in the tunnel [40]. Due to the relationship with the pressure gradient of the initial compression wave at the tunnel exit, the MPW outside the tunnel exit is also symmetrical, as shown in Figure 7. So, the results at the monitoring points on only one side ($T1$, $M1$, and $M3$) are considered in the subsequent discussion.

4.2. Influence of Linings Position and Quantity. The compress wave and MPW characteristics caused by a train passing through tunnels with normal linings and various numbers of segmented linings at different positions with a speed of 350 km/h are studied by numerical simulation.

For the normal linings located at the tunnel entrance, middle, and exit, the maximum values of pressure gradient at $T1$ and MPW at $M1$ and $M3$ are shown in Table 3. It can be found that both the pressure gradient and MPW increase compared to that without linings, which has an adverse effect on the aerodynamics of the tunnel. When the linings are located at tunnel middle and exit, the pressure gradient and MPW decrease compared to that without linings and a favorable effect is induced. The results also show that the mitigation effect on MPW is better when the linings are located near the tunnel exit.

The MPW at $M1$ and $M3$ when the trains travel through the tunnel with different numbers of segmented linings at different positions are shown in Figures 8 and 9, respectively.

It can be seen that the influence of the lining's position on MPW is basically the same for both normal linings and the different number of segmented linings. That is, the linings close to the tunnel middle and exit have a favorable effect on the mitigation of MPW, while an adverse effect will be induced when the linings locate near the entrance of the tunnel.

The amplitude values of MPW at 20 m and 50 m away from the tunnel exit are listed in Tables 4 and 5, respectively. It can be found that when the linings are located at the tunnel entrance and middle, the MPW generated by the tunnel with segmented linings decrease compared to that with normal linings. For the segmented linings locate at the middle and exit of the tunnel, the mitigation effects on the micropressure wave increase with the segment numbers due to the increscent dissipation effect caused by the linings. The amplitude values of MPW at $M1$ and $M3$ are 82.172 Pa and 35.096 Pa when a 30-segment lining is set at the tunnel exit, which is 4.789% and 5.277% lower than that of the tunnel without linings.

However, when the segmented linings are located at the tunnel entrance, the amplitude value of MPW increases gradually with the number of segments. The reason is that the shrinking section of the lining gets closer to the tunnel entrance as the increase of the segmented number and the compression effect of the air is dominant compared to the dissipation effect, which has an adverse impact on MPW. Therefore, the adverse effect of the linings located at the tunnel entrance can be reduced by a small number of segments. When a 10-segment lining is set at the entrance of the tunnel, the amplitude values of MPW at $M1$ and $M3$ are 91.225 Pa and 39.181 Pa, which are 5.701% and 5.749% higher than that of the tunnel without linings but decrease by 6.884% and 6.699% compared to that of the tunnel with normal linings.

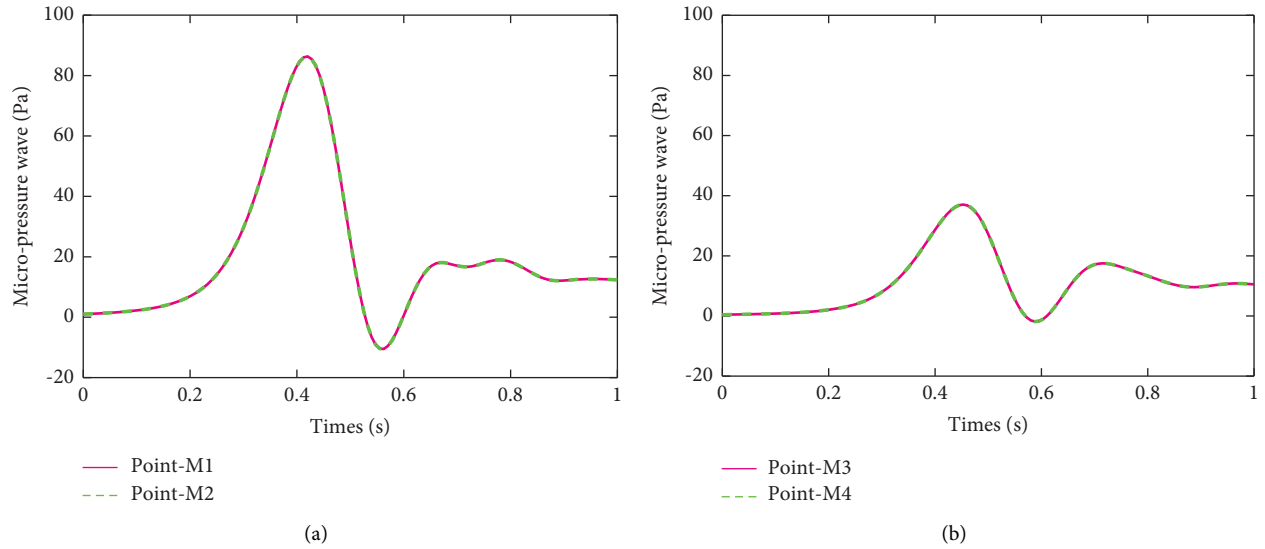

Figure 7: Comparison of micropressure wave in the same plane. (a) 20 m outside the tunnel exit. (b) 50 m outside the tunnel exit.

Table 3: The maximum pressure gradient and micro-pressure wave.

The position of the linings	Without linings	Entrance of the tunnel	Middle of the tunnel	Exit of the tunnel
$(\partial P/\partial t)_{max}$ at $T1$ (kPa/s)	10.49	12.06	10.43	11.20
MPW at $M1$ (Pa)	86.31	97.97	85.89	85.26
MPW at $M3$ (Pa)	37.05	42.00	36.92	35.05

4.3. Influence of Linings Thickness. The influence of the thickness of the linings on MPW is also studied. The aerodynamics caused by a train passing through the tunnel with normal and 10-segment linings of various thicknesses located at the middle of the tunnel is simulated by numerical methods.

The variations of MPW at 20 m and 50 m away from the tunnel exit are shown in Figures 10 and 11, respectively. The results show that MPW decrease slightly with the increment of linings thickness in a certain range for both normal linings and segmented linings due to the increscent dissipation effect.

The amplitude values of MPW at $M1$ and $M3$ are also given in Tables 6 and 7. It can be found that the amplitude values of MPW at two monitoring points drop by 0.629% and 0.707% when the thickness of the segmented linings changes from 0.4 m to 0.6 m.

Thus, the thickness of the lining structure can be designed according to the requirements of structural strength in engineering practice and a thick lining can be used as the cost allows to alleviate the MPW problem outside the tunnel exit.

4.4. Influence of Linings Type. The previous studies show that an effect is induced by the segmented linings located at the tunnel entrance and exit. The aerodynamics of the segmented linings with different types located at the tunnel middle and exit are simulated to study the influences of the linings type on MPW.

As shown in Figure 12, Type 1 denotes the segmented linings start with a constant section compared to the tunnel, while Type 2 denotes the segmented linings start with a constricted section, and 10 segments are set for both types with a thickness of 0.5 m.

When a train travels through the tunnels with different types of segmented linings, the MPW at 20 m and 50 m away from the tunnel portal are given in Figures 13 and 14, respectively.

It has shown quite a difference between the two types of segmented linings located at the entrance of the tunnel. For the segmented linings that start with a constant section (Type 1), the rising of the initial compression wave is divided into two stages, resulting in decreases in pressure gradient and MPW. While the segmented linings start with a constricted section (Type 2), the compression effect is enhanced due to the reduction of the clearance area of the tunnel entrance, which has an adverse on the micropressure wave. The amplitude values of MPW at the $M1$ and $M3$ are 95.787 Pa and 41.06 Pa, respectively, which are 4.999% and 4.796% higher than that with Type 1.

However, the results show little difference between the two types of segmented linings located at the exit of the tunnel. For the segmented linings end with constricted section (Type 1), the mitigation effect is better due to a smaller clearance area at the tunnel exit, as shown in equation (6). The amplitude values of MPW at the $M1$ and $M3$ are 83.204 Pa and 35.569 Pa, which are 0.375% and 0.829% smaller than that with Type 2.

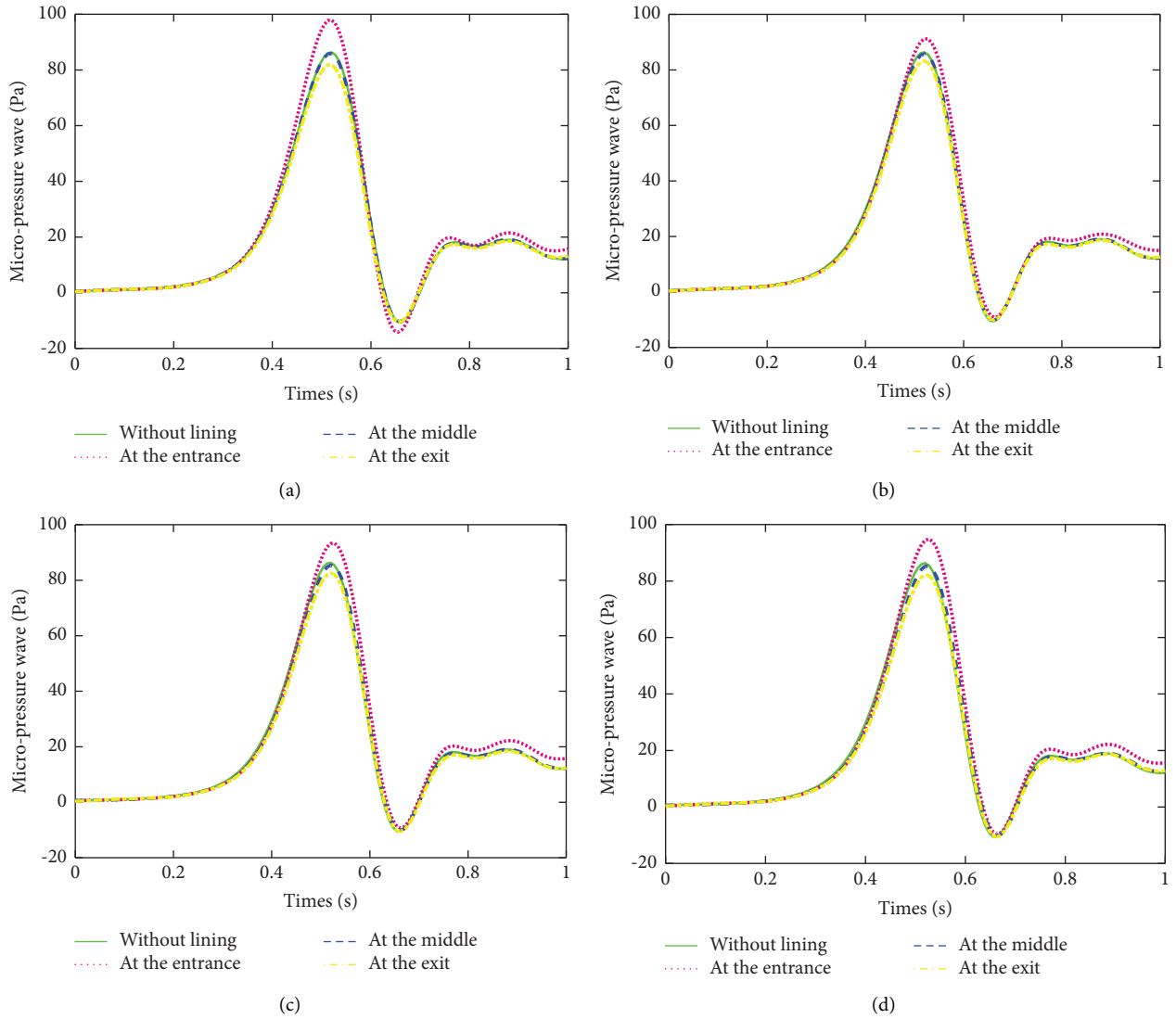

Figure 8: Comparison of the micro-pressure wave at $M1$. (a) Normal linings. (b) 10-segment linings. (c) 20-segment linings. (d) 30-segment linings.

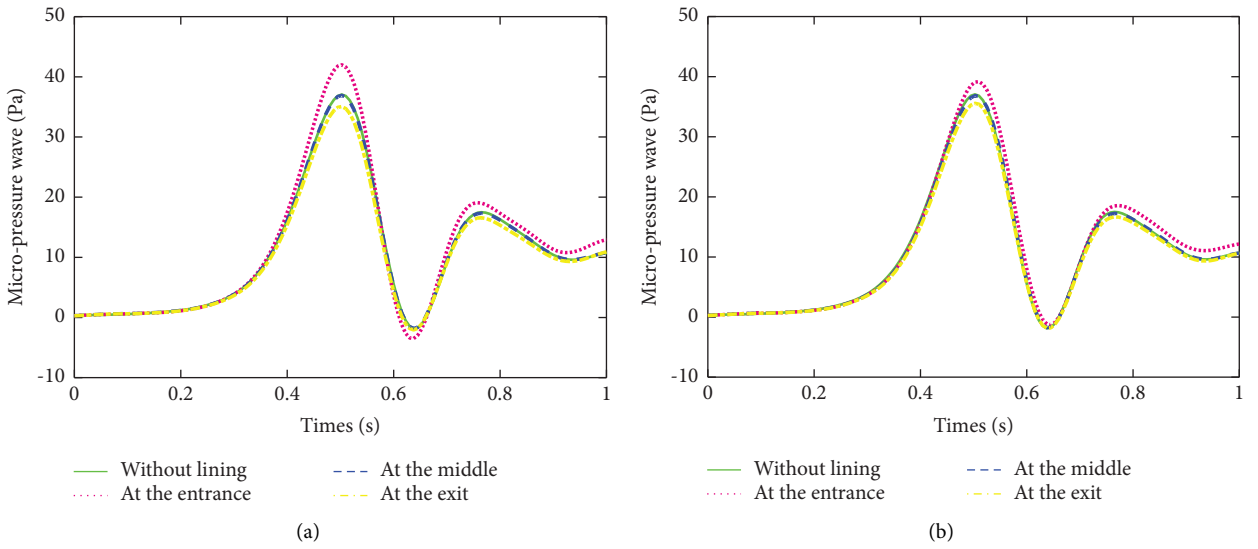

Figure 9: Continued.

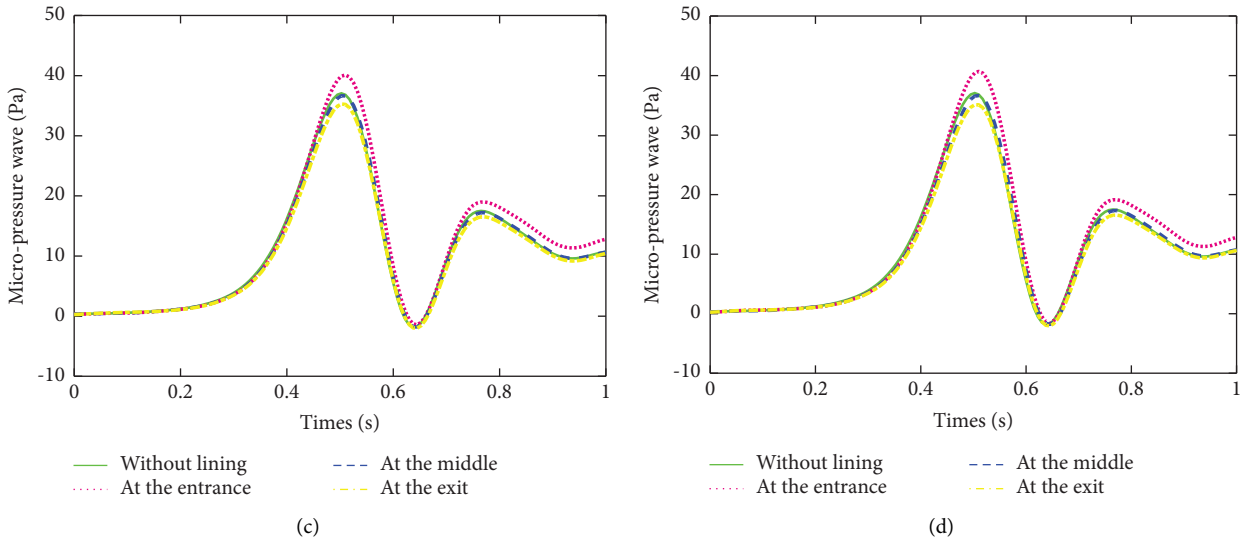

Figure 9: Comparison of the micropressure wave at $M3$. (a) Normal linings. (b) 10-segment linings. (c) 20-segment linings. (d) 30-segment linings.

Table 4: The amplitude values of the micro-pressure wave at $M1$.

The position of the linings	Without linings	Normal linings	Segmented linings		
			10-segment	20-segment	30-segment
Entrance of the tunnel		97.969	91.225	93.417	94.880
In the middle	86.305	85.888	85.769	85.440	85.258
In the exit		81.853	83.204	82.559	82.172

Table 5: The amplitude values of the micro-pressure wave at $M3$.

The position of the linings	Without linings	Normal linings	Segmented linings		
			10-segment	20-segment	30-segment
Entrance of the tunnel		41.994	39.181	40.105	40.701
In the middle	37.051	36.918	36.835	36.655	36.645
In the exit		35.053	35.569	35.286	35.096

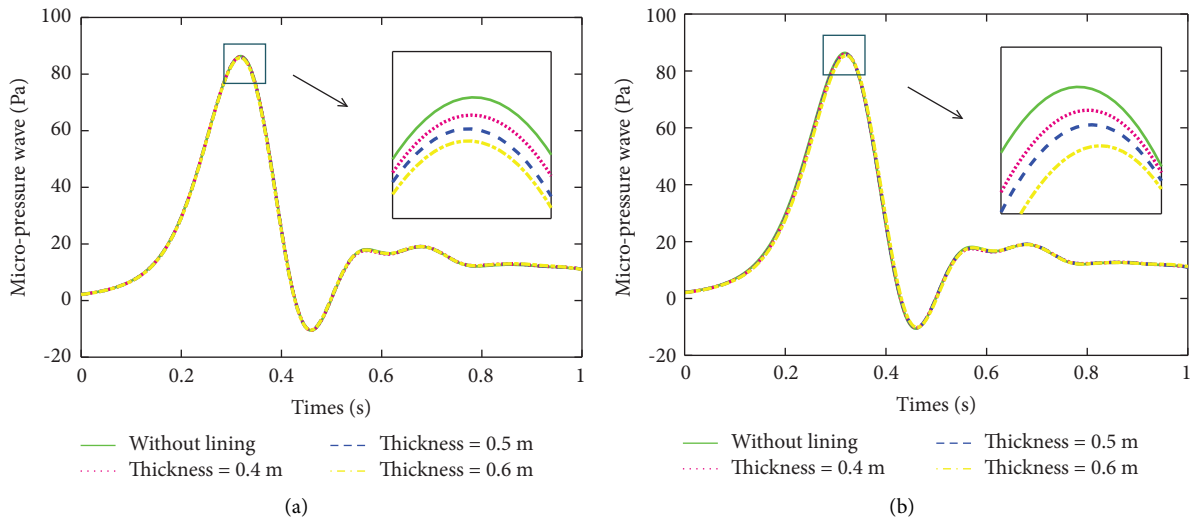

Figure 10: Comparison of the micropressure wave at $M1$. (a) Normal linings. (b) 10-segment linings.

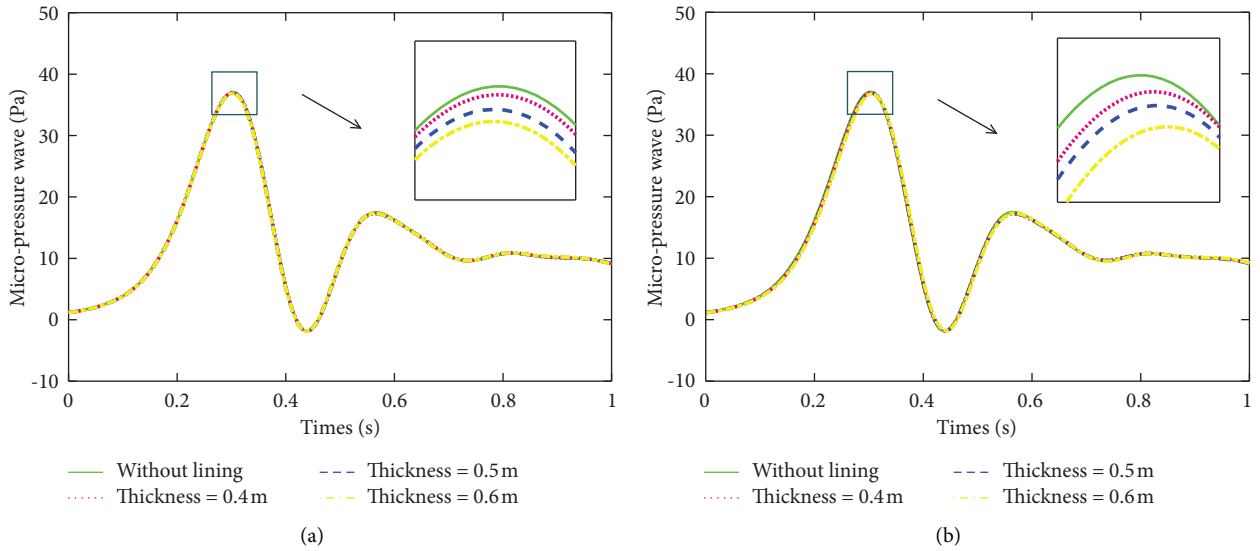

Figure 11: Comparison of the micropressure wave at $M3$. (a) Normal linings. (b) 10-segment linings.

Table 6: Comparison of amplitude values of the micropressure wave at $M1$.

MPW (Pa)	The thickness of linings (m)			
	0 m	0.4 m	0.5 m	0.6 m
Normal linings	86.305	86.076	85.888	85.741
Segmented linings		85.985	85.769	85.444

Table 7: Comparison of amplitude values of the micropressure wave at $M3$.

MPW (Pa)	The thickness of linings (m)			
	0 m	0.4 m	0.5 m	0.6 m
Normal linings	37.051	37.003	36.918	36.850
Segmented linings		36.933	36.835	36.672

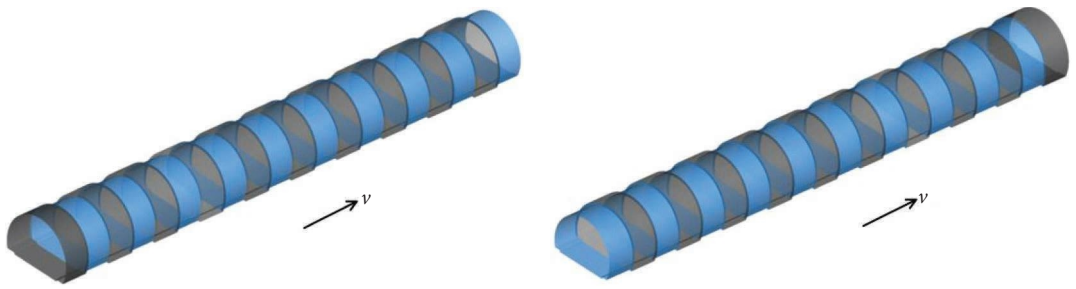

Figure 12: Different types of lining models. (a) Type 1. (b) Type 2.

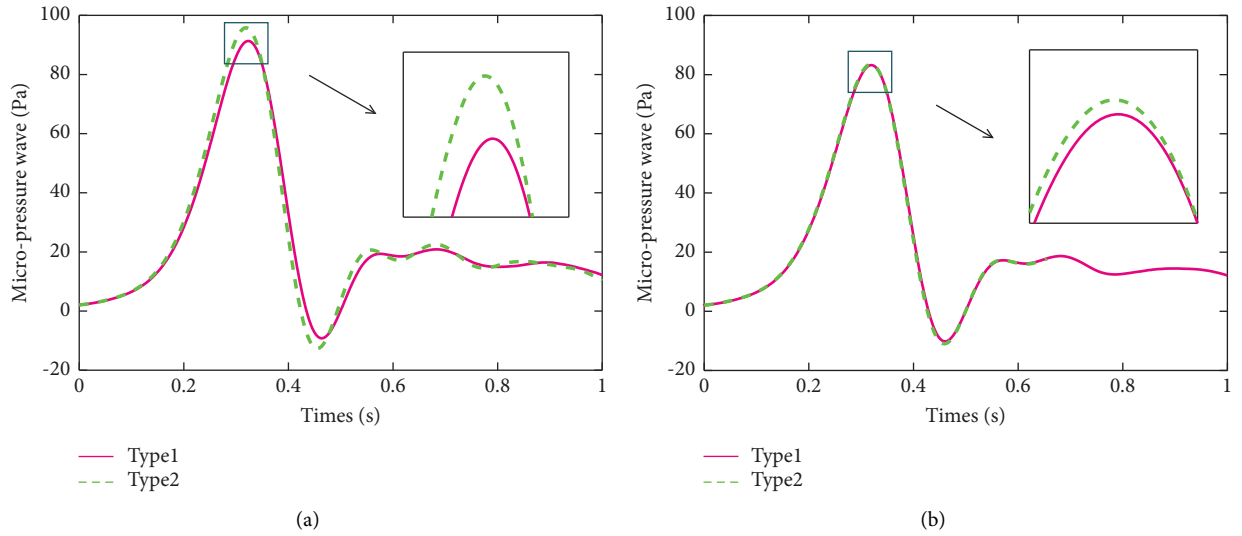

Figure 13: Comparison of the micropressure wave at $M1$. (a) Linings at the tunnel entrance. (b) Linings at the tunnel exit.

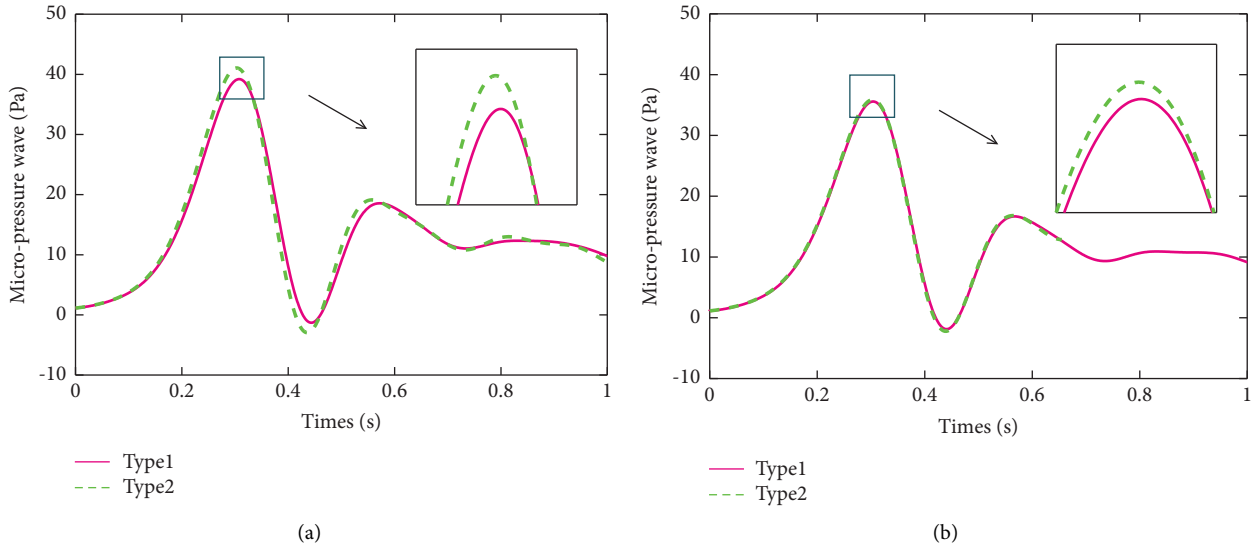

Figure 14: Comparison of the micropressure wave at $M3$. (a) Linings at the tunnel entrance. (b) Linings at the tunnel exit.

The results show that the type of segmented linings located at tunnel entrance has a greater impact on MPW. Therefore, a segmented lining structure can be used if damages occur close to the tunnel entrance, and the constricted section of the lining should be slightly away from the tunnel entrance.

5. Conclusions

In this paper, a 3D numerical method is used to research the aerodynamic impacts produced by trains traveling through a tunnel with linings at 350 km/h. The influence of the numbers, thickness, location, and types of the segmented lining structure on MPW are analyzed. The following can be concluded from the results:

(1) Both normal linings and segmented linings located at the entrance of the tunnel have an adverse effect on MPW, while a favorable effect is induced when the linings locate at the middle and exit of the tunnel and the mitigation effect is better for the linings at the tunnel exit.

(2) When the segmented linings are located at the tunnel entrance, the amplitude of MPW increases with the increase of the number of segments. When the segmented linings are located at the middle and exit of the tunnel, the amplitude of MPW decreases with the increase of the number of segments. In addition, when the linings are located in the tunnel middle, the segmented linings have a better mitigation effect on MPW than the normal linings, which increases with

the segment number of the linings. When a 30-segment lining structure with a thickness of 0.5 m is set near the exit of the tunnel, the amplitude values of MPW at 20 m and 50 m outside the tunnel decrease by 4.789% and 5.277%, respectively;

(3) The mitigation effects of both normal linings and segmented linings increase slightly with the thickness of the linings.

(4) When the damage occurs near the entrance of the tunnel, a segmented lining structure can be used to reduce its adverse effect on MPW and the constricted section of the lining structure should be slightly away from the tunnel entrance.

(5) The problem of tunnel damage can be repaired by adding segmented linings and reducing MPW. Other aerodynamic effects caused by train tunnel (such as train wind, transient pressure, passenger comfort, and so on) will be studied in future work.

Data Availability

All data generated or analyzed during this study are included in this article and are available upon request by contact with the corresponding author.

Conflicts of Interest

The author declares that there are no conflicts of interest.

Acknowledgments

This work was supported by the State Key Laboratory for Track Technology of High-Speed Railway (Grant no. 2021YJ056) and Natural Science Foundation of Shandong Province, China (Grant nos. ZR2020MA057 and ZR2021QE108), and Science and Technology R&D Program of China Railway (P2021G053).

References

[1] T. Miyachi, "Acoustic model of micro-pressure wave emission from a high-speed train tunnel," *Journal of Sound and Vibration*, vol. 391, pp. 127–152, 2017.

[2] D. Uystepruyst, M. William-Louis, and F. Monnoyer, "3D numerical design of tunnel hood," *Tunnelling and Underground Space Technology*, vol. 38, pp. 517–525, 2013.

[3] T. Aoki, K. Matsuo, and H. Hidaka, "Attenuation and distorsion of propagating compression waves in a high-speed railway model and in real tunnels," *Shock Waves in Condensed Matter and Heterogeneous Media*, vol. 1995, pp. 347–352, 1995.

[4] T. Fukuda, S. Ozawa, M. Iida, T. Takasaki, Y. Wakabayashi, and T. Miyachi, "Propagation of compression wave in a long tunnel with slab tracks," *Quarterly Report of RTRI*, vol. 46, no. 3, pp. 188–193, 2005.

[5] L. H. Xu and M. Ma, "Dynamic response of the multilayered half-space medium due to the spatially periodic harmonic moving load," *Soil Dynamics and Earthquake Engineering*, vol. 157, Article ID 107246, 2022.

[6] M. Ma, M. H. Li, X. Y. Qu, and H. G. Zhang, "Effect of passing metro trains on uncertainty of vibration source intensity: monitoring tests," *Measurement*, vol. 193, Article ID 110992, 2022.

[7] C. Zou, J. A. Moore, M. Sanayei, Z. Tao, and Y. Wang, "Impedance model of train-induced vibration transmission across a transfer structure into an overtrack building in a metro depot," *Journal of Structural Engineering*, vol. 148, no. 11, 2022.

[8] M. Bellenoue, B. Auvity, and T. Kageyama, "Blind hood effects on the compression wave generated by a train entering a tunnel," *Experimental Thermal and Fluid Science*, vol. 25, no. 6, pp. 397–407, 2001.

[9] W. Li, T. Liu, X. Huo, Z. Chen, Z. Guo, and L. Li, "Influence of the enlarged portal length on pressure waves in railway tunnels with cross-section expansion," *Journal of Wind Engineering and Industrial Aerodynamics*, vol. 190, pp. 10–22, 2019.

[10] R. Gawthorpe, "Pressure effects in railway tunnels," *Rail International*, vol. 31, pp. 10–17, 2000.

[11] D. Cross, B. Hughes, D. Ingham, and L. Ma, "A validated numerical investigation of the effects of high blockage ratio and train and tunnel length upon underground railway aerodynamics," *Journal of Wind Engineering and Industrial Aerodynamics*, vol. 146, pp. 195–206, 2015.

[12] J. M. Rivero, E. González-Martínez, and M. Rodríguez-Fernández, "A methodology for the prediction of the sonic boom in tunnels of high-speed trains," *Journal of Sound and Vibration*, vol. 446, pp. 37–56, 2019.

[13] M. Ito, "Improvement to the aerodynamic characteristics of Shinkansen rolling stock," *Proceedings of the Institution of Mechanical Engineers - Part F: Journal of Rail and Rapid Transit*, vol. 214, no. 3, pp. 135–143, 2000.

[14] T. Pei, L. Chen, X. Shi, and Y. Shi, "Study on treatment measures of cracks in lining of existing railway tunnel," *Railway Engineering*, vol. 2013, no. 04, pp. 76–79, 2013.

[15] H. Jin, Q. Tian, and Z. Li, "Crack development of rebar rust in rubberized concrete using mesoscale model," *Construction and Building Materials*, vol. 321, Article ID 126409, 2022.

[16] H. Jin, J. Su, and C. Zhao, "Relationship between invert-filling disengaging and deformation of shield tunnel using staggered assembled segment," *KSCE Journal of Civil Engineering*, vol. 26, no. 4, pp. 1966–1977, 2022.

[17] X. Xiang, L. Xue, and B. Wang, "Aerodynamic effects of inclined portals on the initial compression wave generated by a high-speed train entering a tunnel," *Journal of Fluids Engineering*, vol. 137, no. 12, Article ID 121104, 2015.

[18] P. Murray and M. Howe, "Influence of hood geometry on the compression wave generated by a high-speed train," *Journal of Sound and Vibration*, vol. 329, no. 14, pp. 2915–2927, 2010.

[19] T. h. Liu, H. q. Tian, and X. f. Liang, "Design and optimization of tunnel hoods," *Tunnelling and Underground Space Technology*, vol. 25, no. 3, pp. 212–219, 2010.

[20] X. Xiang, L. Xue, B. Wang, and W. Zou, "Mechanism and capability of ventilation openings for alleviating micro-pressure waves emitted from high-speed railway tunnels," *Building and Environment*, vol. 132, pp. 245–254, 2018.

[21] D. H. Kim, S. Y. Cheol, R. S. Iyer, and H. D. Kim, "A newly designed entrance hood to reduce the micro pressure wave emitted from the exit of high-speed railway tunnel," *Tunnelling and Underground Space Technology*, vol. 108, Article ID 103728, 2020.

[22] L. Zhang, M. z. Yang, X. f. Liang, and J. Zhang, "Oblique tunnel portal effects on train and tunnel aerodynamics based on moving model tests," *Journal of Wind Engineering and Industrial Aerodynamics*, vol. 167, pp. 128–139, 2017.

[23] M. S. Howe, M. Iida, T. Fukuda, and T. Maeda, "Theoretical and experimental investigation of the compression wave generated by a train entering a tunnel with a flared portal," *Journal of Fluid Mechanics*, vol. 425, Article ID S0022112000002093, 2000.

[24] F. Liu, W. Zhou, J. q. Niu, and J. Zhang, "Impact of increased linings on pressure transients induced by a train passing through a tunnel," *Sustainable Cities and Society*, vol. 45, pp. 314–323, 2019.

[25] F. Liu, S. Yao, J. Zhang, and Y. b. Zhang, "Effect of increased linings on micro-pressure waves in a high-speed railway tunnel," *Tunnelling and Underground Space Technology*, vol. 52, pp. 62–70, 2016.

[26] J. Gao, "Design analysis on reinforcement sleeves for high-speed railway tunnels based on aerodynamic effect," *Railway Quality Control*, vol. 44, no. 01, pp. 40–44, 2016.

[27] X. Shi, J. Wu, X. Leng, and D. Niu, "Influence of added lining on micro pressure wave of high speed railway tunnel portals," *Railway Engineering*, vol. 57, no. 10, pp. 53–55+59, 2017.

[28] T. Wang, X. Han, L. Zhang, B. Qian, Z. Sun, and H. Liu, "Effect of non-circular tunnel linings on pressure transients induced by high-speed train passes through a tunnel based on moving model test," *Journal of Wind Engineering and Industrial Aerodynamics*, vol. 214, Article ID 104649, 2021.

[29] Q. Fang, D. Zhang, Q. Li, and L. N. Y. Wong, "Effects of twin tunnels construction beneath existing shield-driven twin tunnels," *Tunnelling and Underground Space Technology*, vol. 45, pp. 128–137, 2015.

[30] W. Yang, E. Deng, M. Lei, P. Zhang, and R. Yin, "Flow structure and aerodynamic behavior evolution during train entering tunnel with entrance in crosswind," *Journal of Wind Engineering and Industrial Aerodynamics*, vol. 175, pp. 229–243, 2018.

[31] M. Rabani and A. K. Faghih, "Numerical analysis of airflow around a passenger train entering the tunnel," *Tunnelling and Underground Space Technology*, vol. 45, pp. 203–213, 2015.

[32] J. Du, Q. Fang, J. Wang, and G. Wang, "Influences of high-speed train speed on tunnel aerodynamic pressures," *Applied Sciences*, vol. 12, no. 1, p. 303, 2021.

[33] M. Shao, C. Ma, and S. Hu, "Effects of time-varying fluid on dynamical characteristics of cantilever beams: numerical simulations and experimental measurements," *Mathematical Problems in Engineering*, vol. 2020, Article ID 6679443, 18 pages, 2020.

[34] T. Wang, C. Hu, and Y. Gong, "Mitigation of micro-pressure wave at 400 km/h railway tunnel exit by oblique enlarged tunnel-hood," *Acta Aerodynamica Sinica*, vol. 39, no. 05, pp. 151–161, 2021.

[35] J. Niu, Y. Sui, Q. Yu, X. Cao, and Y. Yuan, "Numerical study on the impact of Mach number on the coupling effect of aerodynamic heating and aerodynamic pressure caused by a tube train," *Journal of Wind Engineering and Industrial Aerodynamics*, vol. 190, pp. 100–111, 2019.

[36] K. Liu, L. Jing, and M. Ren, "The characteristics of air wave induced by two high-speed trains passing by each other in a tunnel," *Advances in Mechanical Engineering*, vol. 10, no. 3, Article ID 168781401876697, 2018.

[37] L. Zhang, K. Thurow, N. Stoll, and H. Liu, "Influence of the geometry of equal-transect oblique tunnel portal on compression wave and micro-pressure wave generated by high-speed trains entering tunnels," *Journal of Wind Engineering and Industrial Aerodynamics*, vol. 178, pp. 1–17, 2018.

[38] A. Yamamoto, "Micro-pressure wave radiated from a tunnel exit," *Nihon Butsuri Gakkai Haru Bunkakai*, The Physical Society of Japan Spring Meeting), Japan, 1977.

[39] L. Zhang, H. Liu, N. Stoll, and K. Thurow, "Influence of tunnel aerodynamic effects by slope of equal-transect ring oblique tunnel portal," *Journal of Wind Engineering and Industrial Aerodynamics*, vol. 169, pp. 106–116, 2017.

[40] Y. Mei, R. Wang, and J. Xu, "Numerical simulation of initial compression wave induced by a high-speed train moving into a tunnel," *Chinese Journal of Computational Mechanics*, vol. 33, no. 1, pp. 95–101, 2016.